Geologic Records of Net Littoral Drift, Beach Plain Development, and Paleotsunami Runup, North Sand Point, Olympic Peninsula, Washington, USA

Author(s): Curt D. Peterson Virginia L. Butler, James K. Feathers, and Kenneth M. Cruikshank
Source: Northwest Science, 88(4):314-328.
Published By: Northwest Scientific Association
DOI: http://dx.doi.org/10.3955/046.088.0406
URL: http://www.bioone.org/doi/full/10.3955/046.088.0406

Curt D. Peterson[1], Geology Department, Portland State University, 1721 SW Broadway, Portland, Oregon 97207

Virginia L. Butler, Anthropology Department, Portland State University, 1721 SW Broadway, Portland, Oregon 97207

James K. Feathers, Luminescence Dating Laboratory, University of Washington, Box 353412, Seattle, Washington, 98195-3412

and

Kenneth M. Cruikshank, Geology Department, Portland State University, 1721 SW Broadway, Portland, Oregon 97207

Geologic Records of Net Littoral Drift, Beach Plain Development, and Paleotsunami Runup, North Sand Point, Olympic Peninsula, Washington, USA

Abstract

A geologic cross-section was constructed across a narrow late Holocene beach plain in a small southwest-facing pocket beach in North Sand Point, Olympic National Park, Washington, to test hypotheses about net littoral drift, potential tectonic uplift, and paleotsunami runup height. Twenty topographic stations (0–12 m elevation NAVD88) and eight auger core sites (2–5 m depth) were examined to establish the stratigraphic development of the narrow beach plain (120 m width). Existing radiocarbon dates and new optically stimulated luminescence (OSL) analyses were used to establish the onset (~1.5 ka) and termination (~0.6 ka) of net beach progradation, confirming net northward littoral drift in latest Holocene time. The anomalous high elevations of the beach plain resulted from an abandoned foredune ridge (9 m elevation) developed above the prograded beach deposits (6 m elevation). No tectonic uplift is required to account for the beach plain elevations. A fine gravel layer (5–30 cm thickness) draped the top of the dune ridge at 7–9 m elevation, but it is not traced to 11–12 m elevation in the adjacent late Pleistocene terrace. The gravel layer is attributed to catastrophic marine surge deposition (10 ± 0.5 m elevation) from a nearfield or locally produced Cascadia paleotsunami at ~1.3 ka. The short duration of the recorded beach plain progradation (about one thousand years), together with a range of OSL grain bleaching ages (11.1–2.3 ka) that pre-date the beach plain deposition, attest to prior pocket beach instabilities and/or sand recycling in the high wave-energy beaches of the northwest Olympic Peninsula coastline.

Keywords: Pocket beach, progradation, paleotsunami, archaeology

Introduction

In this pilot study we analyze the latest Holocene deposits in a very small pocket beach, North Sand Point, Washington, to test hypotheses regarding net littoral drift, late Holocene beach progradation, and paleotsunami runup in the rugged coast of the Olympic Peninsula (Figure 1). It was not known whether Holocene northward littoral drift of beach sand along the northwest Washington coast (Swartz, 1985; Peterson et al., 2010) had continued until latest Holocene time. It was not known what process led to localized beach progradation or seaward accretion (~120 m seaward distance) and abandonment of a sea cliff terrace archaeological site 45-CA-201 in the North Sand Point beach plain. The archaeological site was occupied from about ~2.3 to ~1.6 thousand years before present (ka) (Wessen, 1993). Paleotsunami runup estimates of at least 10 m elevation had been projected for a large Cascadia paleotsunami at ~1.3 ka in the north-westernmost coast of the Olympic Peninsula (Peterson et al., 2013). However, the runup projections were not confirmed by direct evidence of paleotsunami deposition at the predicted elevations located in the open coast.

In this paper we utilize surveyed topography, sand auger core samples, and bounding geologic dates of beach sand deposits in one cross-section to represent beach plain and foredune ridge development in the North Sand Point pocket beach. Radiocarbon and optically stimulated luminescence

[1]Author to whom correspondence should be addressed: Email: curt.d.peterson@gmail.com

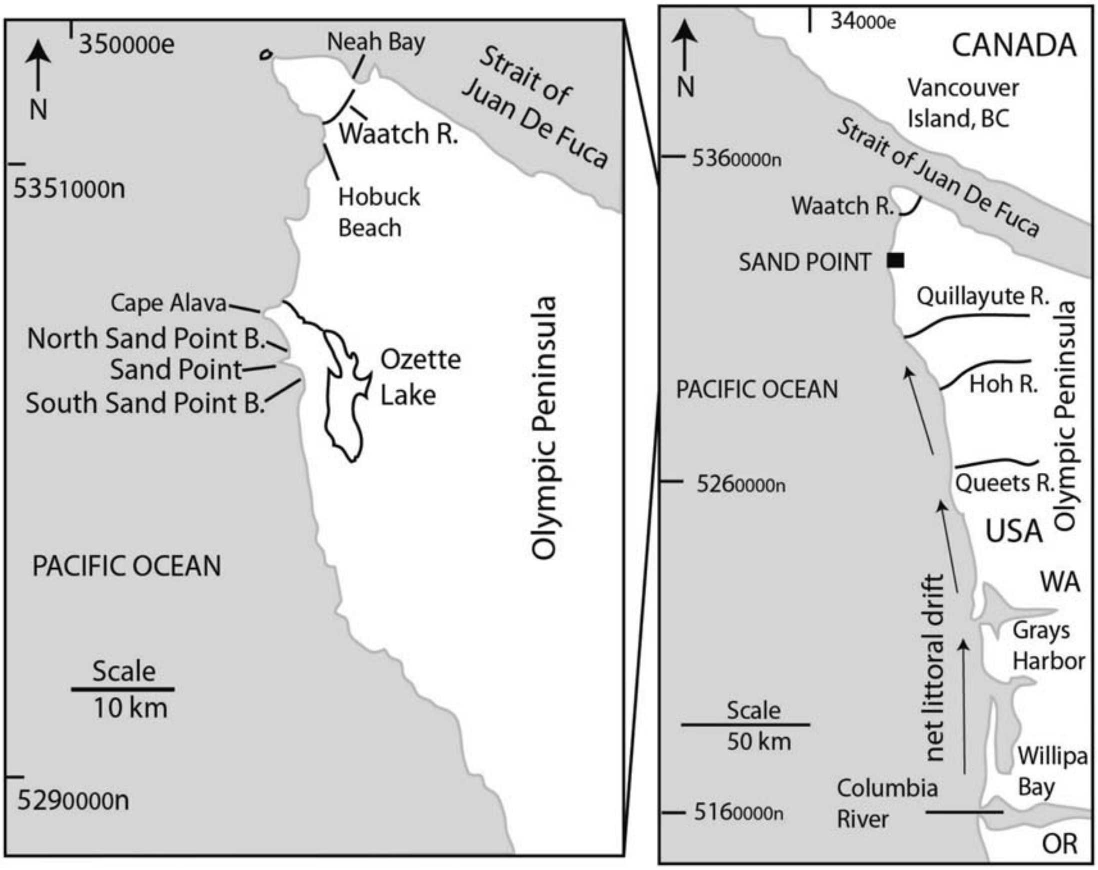

Figure 1. Location of North Sand Point beach in the Olympic Peninsula of Northwest Washington. Net northward littoral drift (arrows) is indicated by beach sand accumulation on the south side of headlands (Swartz, 1985) and by Columbia River sand mineralogy traced north on the inner continental shelf (Peterson et al., 2010). Map coordinates are in meters UTM easting (e) and northing (n). Study area (solid square) shows study locality at Sand Point (see inset).

(OSL) dating of the beach deposits indicate that beach sand progradation was underway by ~1.5–1.3 ka at the back edge of the narrow beach plain. A stratified beach gravel deposit that mantles the crest of a foredune sand ridge (9 m elevation) in the narrow beach plain is attributed to paleotsunami runup from a great Cascadia earthquake. Ranges of OSL ages from minor components of the beach sand in the prograded beach deposits indicate a complex history of sand supply and remobilization in the high-energy coastline of the Olympic Peninsula. These findings should motivate more comprehensive geomorphic studies of remote pocket beaches in the west coast of the Olympic Peninsula.

Background

Swartz et al. (1985) used beach sand accumulations that were located on the south sides of small headlands in the Olympic Peninsula (Figure 1) to predict conditions of net northward littoral sand transport during late Holocene time. Peterson et al. (2009) similarly used the positions and ages of coastal sand dune deposits in subcell embayments to both establish the direction and timing of net littoral sand drift along the US West Coast. At the time of the Peterson et al. (2009) littoral drift study it was not known that small foredune ridges were locally preserved in small pocket beaches in the remote coastline of the Olympic National Park. Could such small pocket-beach deposits be dated to confirm net northward littoral sand drift along the otherwise rocky shoreline? Such evidence could extend the regional littoral sand drift analyses to the north-westernmost extent of the Washington coast.

The rugged coastline of the northwest Olympic Peninsula (Figure 1) has been attributed to reactivation of ancient thrust faults (Snavely et al., 1986), Quaternary tectonic uplift of the Olympic Range (Pazzaglia and Brandon, 2001), and post-glacial isostatic uplift in the Strait of Juan de Fuca (Mosher and Hewitt, 2004). Those factors likely fueled speculations including 1) substantial uplift of marine terraces in late Quaternary time (West and McCrumb, 1988), 2) uplift of beach platforms in late Holocene time (Bird and Swartz, 2000) and/or 3) coseismic uplift of shorelines during great Cascadia earthquakes.

Regional compilations of dated marine terrace elevations (Marine Isotope Stage 5 or MIS5) along the central-west coast of the Olympic Peninsula (Figure 1) have demonstrated only modest uplift (generally < 10 m MSL) since 80–130 ka (Huesser, 1977; Thackray, 1998). Reports of uplifted Holocene beach platforms at the northwest end of the Olympic Peninsula (Bird and Swartz, 2000) have yet to be confirmed by dated beach-platform deposits. Investigations of tidal marsh records in the Waatch Valley wetlands did not find evidence of coseismic uplift events during the last several ruptures (~1.3-0.3 ka) of the Cascadia megathrust or subduction zone fault (Peterson et al., 2013). Given the uncertainties of long-term uplift rates or coseismic uplift events in the west coast of the Olympic Peninsula, as outlined above, the potential for regional uplift producing a raised beach platform at North Sand Point (Wessen, 1993) was left unresolved.

Overland runup distances of the last several Cascadia paleotsunamis have been mapped in supratidal wetlands in the Waatch Creek valley (Figure 1) at the northwestern end of the Olympic Peninsula (Peterson et al., 2013). Inundation distances, as based on anomalous beach sand and/or marine diatom indicators, ranged from 1 to 4.5 km from the present shoreline. The largest recorded runup event in Waatch Creek valley was dated to the regional Cascadia rupture at ~1.3 ka. The paleotsunami wave height was projected to have reached 11.5 m elevation at the open coast or modern shoreline. The predicted shoreline runup height was based on 1) an inland deposit elevation of 2.5 m and 2) landward attenuation of 3 m km^{-1} over an inundation distance of 3.0 km from the paleo-shoreline at ~1.3 ka. Unfortunately, no upland depositional settings were observed at the mouth of the Waatch Creek to verify the projected paleotsunami runup elevations at the open coast shoreline in northwest Washington.

A field investigation of prograded beach deposits, about 120 m in width, in the North Sand Point beach plain (Figure 1) was conducted to test whether the abandonment of an adjacent Native American archaeological site 45-CA-201 on a sea cliff terrace edge (Wessen, 1984) was coeval with the onset of beach progradation. Latest occupation of the midden was dated at ~1.6 ka (Table 1). Radiocarbon dates from a buried charcoal sample that was collected at the landward end of the beach plain yielded an age of ~1.5 ka. The seaward end of the profile is dated by a whale bone at about 650 yr BP (~0.7 ka) that was collected from a surface midden in the back-edge of the modern beach (Paul Gleeson, Olympic National Park, personal communication, 2008). Although the archaeological site abandonment was tentatively tied to the onset of beach deposit progradation in the North Sand Point embayment (~1.5 ka) it was not established whether the onset of beach progradation was forced by tectonic uplift, post-glacial isostatic uplift, or by some other process (Gary Wessen, Wesson & Associates, personal communication, 2010).

Methods

This field study focused on a geologic cross-section that traversed the prograded Holocene beach plain (400 m in length north-south and 120 m in width east-west) within the North Sand Point beach segment (Figure 2). This was the only cross-section that was permitted by the US National Park Service in the vicinity of the Native American occupation site 45-CA-201 within the North Sand Point wilderness coastline in the

TABLE 1. Radiocarbon dated samples from the North Sand Point locality.

Site	^{14}C Date yr BP/(ka)	Sample #	Comments
45-CA-201	1,600 ± 75 / (~1.6)	SI - 4366	Charcoal from top of shell midden component
45-CA-201	2,270 ± 75 / (~2.3)	SI - 4367	Charcoal from base of shell midden component
Atwater93	1,550 ± 80 / (~1.5)	Beta57566	Wood from east end of beach plain
GleesonWB	650 ± 60 / (~0.7)		Whale bone from west end of beach plain

Radiocarbon data for 1) archaeology site 45-CA-201 is from Wesson (2003), 2) Atwater93 is from Atwater (unpublished data, 1993; personal communication to G. Wessen, 1993), and 3) GleesonWB is from Paul Gleeson (Olympic National Park, personal communication, 2008). Radiocarbon ages are rounded to 0.1 thousand years before present (x.x ka) for approximate comparisons to luminescence ages presented in this study.

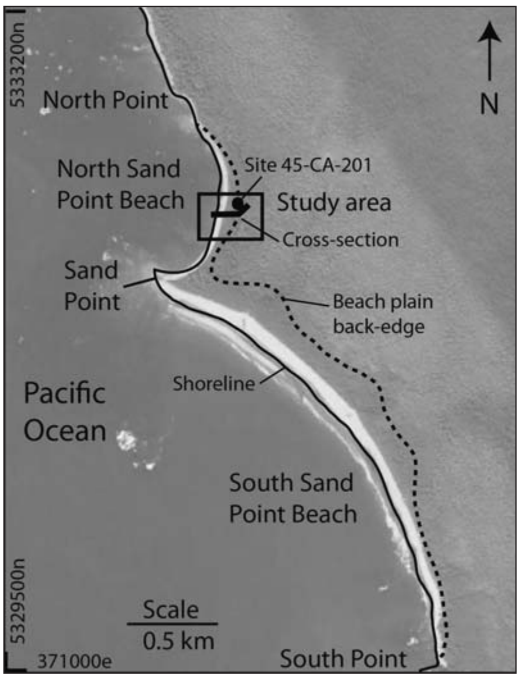

Figure 2. Location of study area (boxed) in North Sand Point pocket beach. The single study cross-section (bold line) extends from the modern shoreline (narrow bold line) to the back-edge of the beach plain (dashed line) at about 12m NAVD88. OSL sample sites are from the west end and east end of the beach profile.

Olympic National Park. The cross-section was contained within an across-shore topographic profile (160 m length) that extended eastward from the shoreline at mean lower low water (MLLW) to late Pleistocene terraces at 9–12 m elevation.

The small pocket beach is located on the south side of a prominent headland complex, Alava Point (Figure 1) that partially trapped northward moving sand in several linked pocket beaches on either side of Sand Point. In this study we use the North American Vertical Datum of 1988 (NAVD88) to establish elevation. The 0 m NAVD88 datum is about one meter below local mean sea level (MSL) or about equivalent to mean low low water (MLLW) in the study area.

Profile endpoint geo-referencing in North Sand Point was established with a 12-channel real-time WAAS-assisted GPS (estimated horizontal error ± 5 m) (Figure 2). Topographic surveying was completed with an electronic distance measuring (EDM) total station, 1 arc second theodolite. Horizontal and vertical errors in the North Sand Point profile are estimated to be ±1.0 cm relative to the local elevation datum control point. The local datum was surveyed into mean tidal level, as based on mid-swash sea level surveys taken over two tidal cycles during calm surf conditions (date July 27, 2010). The local elevation datum in the North Sand Point profile was tied to the regional NAVD88 datum via concurrent tide level curves, as shot from the North Sand Point profile and from a GPS base station (NOAA E4-GPS-BBCJ13) at nearby Hobuck Beach (Figure 1) (Peterson et al., 2013). Regional datum control error for the North Sand Point profile is estimated to be ± 0.25 m. The total 0.5 m error is based on ¼ resolution of the predicted tidal range (~2 m). The mean tide position (1 ± 0.25 m NAVD88) at the North Sand Point beach face (SS1) was surveyed into a stable landward control site SS8 (UTM-10N coordinates of 373011 m E and 5332156 m N) with a sea level calibrated elevation of 5.2 ± 0.25 m NAVD88 for ground level (Figure 3).

Auger coring for sediment textural analysis was performed with a Dormer sand auger (7.5 cm diameter) at eight core sites in a shore-perpendicular cross-section (Figure 2). Paired core sites (SP1 and SP2 and SP3 and SP4) were collected at opposite ends of the cross-section to test for local variability and to predict optimal lithology for OSL sampling. Recovered core deposits were logged at 10–20 cm depth intervals. Auger core depths (3–5 m below ground surface) were limited by refusal in basal beach cobble. A bedrock beach platform (2–4 m elevation NAVD88) was traced between local shoreline exposures at Sand Point and North Point. The uplifted bedrock platform is overlain by outwash deposits of silty sand and subangular gravel at the back-edge of the North Sand Point beach plain. A thin loess cap (10–30 cm thickness) mantles the glacial outwash terrace at the landward end of the North Sand Point topographic profile (Peterson et al., 2014). The loess cap was examined for beach-rounded pebbles, as possible tracers of paleotsunami inundation, in shallow hand-dug test pits (25 x 25 x 25 cm).

Mean grain sizes of the sand size fractions in the beach and foredune deposits were visu-

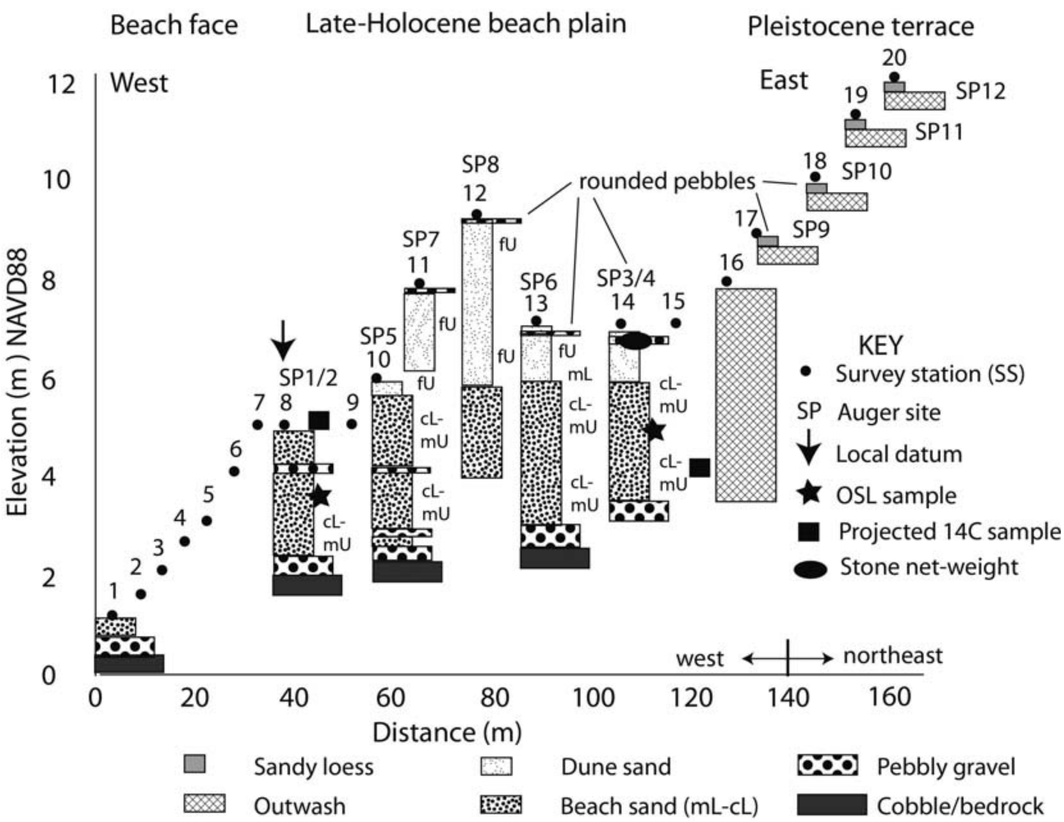

Figure 3. Survey stations (SS) and auger core logs (SP) are shown for the North Sand Point cross-section. The cross-section local datum (SS8) was tied to the NAVD88 elevation datum by surveyed sea levels. Deposit grain size was visually calibrated at 10–20 cm drive intervals, including the following size classes: coarse lower (cL), medium upper (mU), medium lower (mL), and fine upper (fU). Optically stimulated luminescence (OSL) samples were taken at sites SP2 and SP4 (Table 3). Previously reported radiocarbon dates, from an adjacent cross-section (Atwater, unpublished data, 1993; Wessen, 1993), are projected into approximate corresponding positions in this North Sand Point cross-section.

ally estimated and recorded at 10–20 cm auger depth intervals in the field with a CANAM grain size card as follows: vcU (1410–2000 μm), vcL (1000–1410 μm), cU (710–1000 μm), cL (500–710 μm), mU (350–500 μm), mL (250–350 μm), fU (177–250 μm), fL (125–177 μm), fvU (88–125 μm), and vfL (62–88 μm). Laboratory mechanical sieving was used for quantitative analysis of mean and standard deviation of sand fractions in representative samples. Pebble sizes in the paleotsunami gravel layer were digitally measured by outline against a 1x1 mm background grid, to establish intermediate diameter in millimeters (mm). Pebble rounding was visually estimated from a relative rounding scale, including the following intervals: angular, subangular, subrounded, rounded and well-rounded (CANAM grain size card).

OSL dating was performed on two beach sand samples taken from the North Sand Point cross-section (Figure 2) to confirm the onset and duration of beach deposit accretion, as indicated by previous radiocarbon dating in the study area (Brian Atwater, unpublished data, 1993; Wessen, 2003). The landward OSL sample (UW2470) was taken in the prograded beach deposits at a subsurface depth of 2.4 m depth in core site SP3. The SP3 core site was located about 20 m distance seaward of the base of the abandoned sea-cliff terrace riser. The UW2470 OSL sample age should post-date the onset of beach accretion at the North Sand Point cross-section. The seaward OSL sample (UW2469) was obtained in beach sand deposits at a subsurface depth of 1.3 m in SP2. The SP2 core site is located about 20 m landward from the modern beach face. The UW2469 OSL sample should date the last stage(s) of net beach accretion in the North Sand Point beach plain. OSL analyses of individual K feldspar grains (180–212 μm size range), including 69 suitable grains from sample UW2470 and 81 suitable grains from sample UW2469, permitted the discrimination of different populations of grain OSL ages within each sample. Details about the laboratory procedures used for the OSL dating of the North Sand Point beach samples are provided elsewhere (Feathers and Sheikh, 2012).

Results

Topographic Profile

The narrow beach plain at North Sand Point is characterized by one shore-normal cross-section in this study (Figure 2). The North Sand Point cross-section was anchored at the modern shoreline (SS1) at mean tidal level (1.0 ± 0.25 m NAVD88). The topographic profile was extended 140 m due east from the modern beach toe to the abandoned sea-cliff in the Pleistocene terrace (SS17) at about 9 m elevation. An intervening shore-parallel sand ridge reached 9 m elevation (SS12) at a distance of about 60 m from the modern beach. The topographic profile was extended an additional distance of 20 m to the northeast of the abandoned sea-cliff to establish the elevations of several stepped surfaces at 10–12 m elevation in the Pleistocene terrace (SS18, SS19, and SS20).

Auger Core Logs

Core logs from SP1/2, SP5, SP8, SP6 and SP3/4 demonstrate the thickness of beach sand (3–4 m thickness) above beach gravel (0.2–4 cm grain size diameter) (Figure 3). About 0.5 m of the basal beach gravel was penetrated in the auger boreholes prior to auger refusal in cobble clasts and/or bedrock at 2–3 m elevation. The beach sand deposits, in the medium-upper to coarse-lower grain size ranges (mU-cL), are overlain by dune sand (0.5-3.1 m thickness) in the fine-upper to medium-lower (fU-mL) grain size ranges. One thick layer (20 cm thick) of pebbles (2–3 cm diameter) in framework support was encountered in SP1/2, at 0.6–0.8 m depth. The pebble layer showed a sharp lower contact with underlying beach sand. Another anomalous layer of gravel (15 cm thick) was encountered at about 1.5 m depth in SP5.

An anomalous layer of fractured and baked rock fragments, apparently fire cracked rock (FCR), occurred at 0.85–0.90 m depth in SP1/2. The scattered FCR occurred immediately below the anomalous rounded-gravel layer. The largest angular FCR fragments reached 7 cm in maximum length in SP1/2. We presume the FCR material represents past human food processing activities.

No other cultural remains were identified at deeper levels in SP1/2 or SP5. Similar low-density scatters of FCR, sometimes associated with degraded bone and shell, have been found in other testing sites along the coast of Olympic National Park (David Conca, Olympic National Park, personal communication, 2014).

The transition between the coarser beach sand and finer dune sand occurred at 5.5–6.0 m elevation in auger holes SP10, SP8, SP6, and SP3/4. The dune sand section occurs in a narrow ridge (SS10–SS15) so it is referred to here as an abandoned beach foredune ridge. One anomalous gravel layer (5–30 cm thickness) occurred at the top of the foredune sand deposits in SP7, SP8, SP6, and SP3/4 at elevations ranging from 7 to 9 m (Figure 4). The anomalous gravel deposits in SP6, SP7 and SP8 were horizontally plane bedded

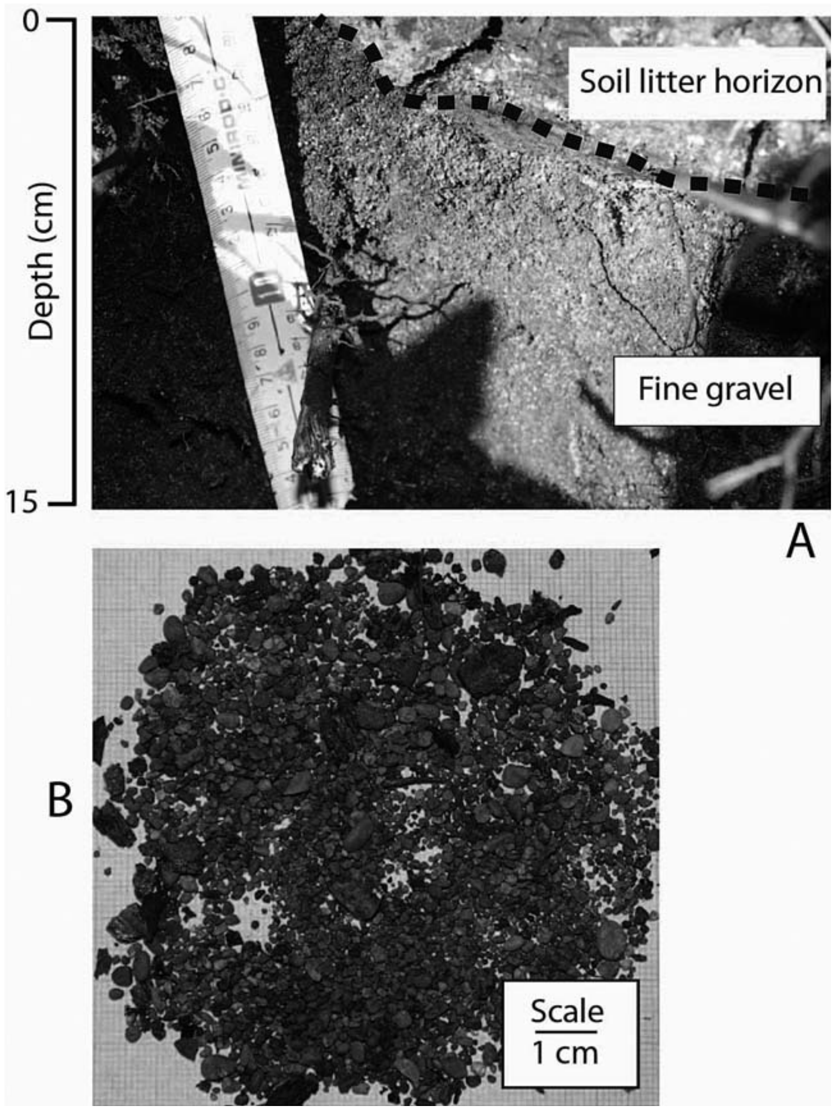

Figure 4. Part A: Anomalous gravel layer (15 cm thickness) at top of auger site SP8. Near-surface gravel layer is overlain by roots and decayed organics in a soil litter horizon. Part B: Bulk sample of the gravel layer from 5–8 cm depth. See Figure 3 for the position of the anomalous gravel layer at the top of core site SP8.

with sharp lower contacts above dune sand. The gravel in SP3/4 was mixed with dune sand (20–30 cm thick layer) and it included a large (20 cm) grooved-stone net weight.

Deposit Grain Sizes

Beach, dune, and anomalous gravel deposits were analyzed for grain-size distributions by mechanical sieving (63–3962 μm size range) and by digitization of small pebbles (4–20 mm diameter range). Modern beach sand from the active beach face at station SS6 (684 ± 637 μm) is easily discriminated from modern dune sand in small dune mounds at station SS10 (207 ± 64 μm), on the basis of both mean size and grain size sorting (Table 2). Prehistoric beach sand deposits in SP1 (846 ± 504 μm), SP2 (421 ± 454 μm) and SP3 (767 ± 929 μm) are also discriminated from overlying dune sand, as analyzed from SP7 (331 ± 51 μm) and SP8 (270 ± 59 μm).

Anomalous gravel deposits at the top of the foredune ridge deposits in SP7 and SP8 were analyzed for 1) mean and standard deviation of the sand and granule size fractions (< 4 mm diameter) and 2) ranges of pebble sizes (> 4 mm diameter) (Table 2). The sand/granule size fractions from SP7 (1792 ± 795 μm) and SP8 (2317 ± 1364 μm) are discriminated from the underlying dune sand populations in terms of both grain population means and variances. The pebble size fractions (> 4 mm diameter) in the anomalous gravel deposits were analyzed for abundance, based on volume point counts, in bulk samples from SP7-TG (35%) and sample SP8-TG (20%). The ranges of pebble sizes (> 4 mm) were based on intermediate diameter (Di) for samples SP7-TG (0.4–15 mm) and SP8-TG (0.4–13 mm). Pebble rounding ranged from rounded to well-rounded, reflecting beach gravel origins. The horizontal plane-bedding of the rounded pebbles represents transport by sustained high-velocity marine surge(s) that exceeded 9.0 m elevation.

Rounded pebbles were rare (2–5% bulk sample volume) in bioturbated sandy-loess deposits on the Pleistocene terrace surfaces at SP9 (size range 0.9–14 mm) and SP10 (size range 0.7–10 mm) (Table 2). As previously noted, no pebbles (> 4 mm diameter) were found in the sandy-loess deposits (~1 kg samples) from SP11 or SP12 at 11–12 m elevation (Figure 3). The minor sand fractions in the bioturbated loess deposits are fine grained (fU-mL). It is not known whether the sand fractions in the bioturbated loess were derived from marine surge or eolian transport.

TABLE 2. Grain size analyses from beach, dune and anomalous gravel layers. Sample depths are in meters (m) below surface. See Figure 3 for survey station (SS) positions and auger core site (SP) locations.

Sample	Depth (m)	Mean (μm)	± 1 Std. Dev. (μm)	Mean SD Norm	Pebble range (mm)
Modern beach SS6	0.0	684	637	0.93	
Modern dune SS10	0.0	207	64	0.31	
SP1-beach	0.5	846	504	0.59	
SP2-1-beach	2.8	421	454	1.08	
SP3-1-beach	3.1	767	929	1.21	
SP7-TG < 4 mm	0.05	1792	795	0.44	
SP7-TG > 4 mm	0.05	—	—	—	0.4–15
SP7-dune	0.5	331	51	0.16	
SP8-TG < 4 mm	0.05	2317	1364	0.59	
SP8-TG > 4 mm	0.05	—	—	—	0.4–13
SP8-dune	0.5	270	59	0.21	
SP9-TG > 4 mm	0.05	—	—	—	0.9–14
SP10-TG > 4 mm	0.05	—	—	—	0.7–10

OSL Ages of Beach Deposits

OSL ages of samples UW2469 in SP2 and UW2470 in site SP4 yield multiple ages for each sample based on different grain populations (Table 3). Central ages of the samples, 2.68 ± 0.29 ka (UW2470) and 1.19 ± 0.12 ka (UW2469), confirm latest Holocene ages for the beach plain. Sample UW2470 from the landward site SP4 is divided into two single-age components. The major component (92% of total grains) provides an age of 2.27 ± 0.28 ka. The minor component (12% of total) provides a pre-Holocene age of 11.2 ± 8.3. The late Pleistocene age (11.2 ka) indicates little or no recent bleaching of a few reworked grains that were supplied to the prograding beach plain. The reworked grains could possibly have originated from eroding outwash deposits in nearby sea cliffs or river cut banks. Sample UW2469 from the seaward site SP2 contains a major component (88% of total grains), which yields an age of 0.98 ± 0.09 ka. The minor component of sample UW2469 provides a much older age of 4.71 ± 1.1 ka. The small number of older grains in the minor component could reflect reworking of late Holocene beach or inner-shelf deposits. The incomplete bleaching of most grains during their recent emplacement in the prograded beach plain could arise from 1) very rapid transport and deposition on a prograding intertidal beach face, 2) grain shadowing in concentrated sheet flow transport and deposition, and/or 3) transport and deposition during night darkness. To reduce bias from reworked grains, either from eroded terrace deposits or remobilized beach/inner-shelf sediments, only the youngest grains in each sample were used to estimate the most recent depositional age. This approach uses the minimum age model, which yielded ages for samples UW2470 and UW2469, respectively, of 1.32 ± 0.19 ka and 0.64 ± 0.09 ka. These minimum ages best represent the emplacement dates of beach deposits at SP4 (1.3 ka) and SP2 (0.6 ka).

Discussion

Timing of Beach Plain Progradation

Minimum OSL ages of beach deposits in SP4 and SP2 confirm the onset and termination ages of beach progradation at North Sand Point, as based on previously reported radiocarbon ages. A radiocarbon age of buried charcoal in beach deposits at the foot of the abandoned sea cliff

TABLE 3. OSL laboratory and age results from North Sand Point beach sand grains.

Dose rate information

Sample	^{238}*U* *(ppm)*	^{233}*Th* *(ppm)*	*K* *(%)*	*Beta dose rate (Gy/ka)* β-counting	α-counting/flame photometry	*Total dose rate** *(Gy ka^{-1})*
UW2469	0.86 ± 0.07	1.55 ± 0.48	0.56 ± 0.03	0.66 ± 0.06	0.61 ± 0.03	1.20 ± 0.12
UW2470	0.98 ± 0.08	1.14 ± 0.40	0.50 ± 0.03	0.59 ± 0.06	0.56 ± 0.03	1.18 ± 0.12

Ages in ka (before 2012)

Sample	*Central age (ka)*	*Ages from finite mixture (ka)* *Component 1*	*Component 2*	*Min. Age (ka)*
UW2469	1.19 ± 0.12	0.98 ± 0.09 (88%)	4.71 ± 1.1 (12%)	0.64 ± 0.09
UW2470	2.68 ± 0.29	2.27 ± 0.28 (92%)	11.2 ± 8.3 (8%)	1.32 ± 0.19

Notes: The two components (1 and 2) represent two single-aged populations using a finite mixture model. The model assumes all values within one component are normally distributed and that single-aged populations have sample-specific characteristic over-dispersion (spread in values beyond what can be accounted for statistically), in this case 35%. The minimum age model represents the youngest age that can be supported statistically. See Galbraith and Roberts (2012) for additional details on these models. Ages are thousand years before present 2012 (ka). Sample positions in soil profiles SP4 (UW2470) and SP2 (UW2469) are shown in Figure 3.

(~1.5 ka) (Brian Atwater, U.S. Geological Survey, unpublished data, 1993) pre-dates the minimum OSL age of 1.32 ± 0.19 ka in SP4 (Figure 3; Table 2). The SP4 core site position was located well seaward (25–30 m distance) of the terrace riser to avoid any contamination from the sloughing of sand grains from the abandoned terrace sea cliff. The minimum OSL age underestimates the age of initial progradation at the foot of the terrace riser, located 25–30 m landward of SP4. For the purposes of this study we defer to the buried charcoal radiocarbon age of 1,550 ± 80 yr BP or 1.4–1.6 ka for the onset of beach plain progradation at North Sand Point (Table 1). The age of abandonment of the archaeological site 45-CA-201 is within the dating range error of the dated onset of beach progradation at North Sand Point, as reported by Wessen (1993). The termination of net sand accumulation in the North Sand Point cross-section is approximated by the minimum OSL date of 0.64 ± 0.09 ka in SP2 (Figure 3). The minimum OSL age at SP2/3 is similar to the reported whale bone age of 650 ± 60 yr BP (no marine reservoir correction) or 0.6–0.7 ka from a midden site that is adjacent to SP1/2.

Causes(s) of Beach Plain Progradation

The onset of beach plain progradation in North Sand Point (~1.5 ka) was not the product of local fault uplift in an active accretionary prism. The anomalous height of the beach plain ridge crest (9 m NAVD88) does not reflect uplift of beach deposits, as previously hypothesized, but rather it is the result of foredune development above prograded beach facies (Figure 3). The eolian dune sand is discriminated from the beach deposit facies on the bases of 1) fine sand size (Table 1) and 2) the lack of pebbles, with the exception of anomalous gravel layers at the top of the dune deposits. The maximum elevations of the beach deposit facies in SP5, SP8, SP6 and SP3/4 (5.5–6.0 m) are similar to the elevation of modern beach overwash deposits at SP8 (5.0 m).

How does the timing of the onset of beach plain progradation in North Sand Point (~1.5 ka) compare to past great earthquake cycles in western Washington? The last four ruptures occurred at 0.3, ~1.1, ~1.3 and ~1.7 ka (Atwater et al., 2004). The first three of those ruptures, and possibly another prior to ~1.1 ka, were recorded by minor coseismic subsidence (0.5–1.0 m) in the Waatch Creek wetlands (Peterson et al., 2013). It is not known if the ~1.7 ka coseismic subsidence event, as recorded in Grays Harbor and Willapa Bay (Atwater et al., 2004), extended north to the Sand Point locality. It predates the reported wetland records in Waatch Creek (Peterson et al., 2013). We can only speculate as to whether coseismic subsidence from a regional ~1.7 ka rupture event could have led to erosion of the North Sand Point pocket beach and whether subsequent interseismic uplift and beach sand recovery could have initiated the progradation at North Sand Point at ~1.5 ka. A ground penetrating radar (GPR) survey of the Hobuck Beach plain at the Waatch Creek mouth demonstrated several very-weak retreat scarp features (Figure 5), but their origins and ages are unknown. It is recommended that such GPR surveys be conducted at the Sand Point beach plains to establish whether any stratigraphic records of coseismic beach retreat events (Meyers et al., 1996) are recorded and preserved there.

Other mechanisms of episodic beach erosion in Pacific Northwest beaches include El Ninos (Peterson et al., 1985), which due to their southerly storm-track trajectories can displace sand to the north (Peterson et al., 1990; Ruggiero et al., 2010a) or even remove sand from small pocket beaches. One alternative explanation to the onset of progradation at North Sand Point is that it does not represent recovery from an erosional event, but rather it reflects initial net entrapment of sand moving northward around Sand Point. However, the lack of net progradation after 0.6 ka in the North Sand Point profile (Figure 3; Table 3) argues against a net surplus of sand supply to the North Sand Point pocket beach in recent times. Progradation ages in other pocket beaches are needed to test regional versus local mechanisms of pocket beach plain development in the Olympic Peninsula.

Cascadia Paleotsunami Runup

The anomalous fine gravel layers at the top of the dune deposits in SP7, SP8, SP6 and SP3/4 (Figures

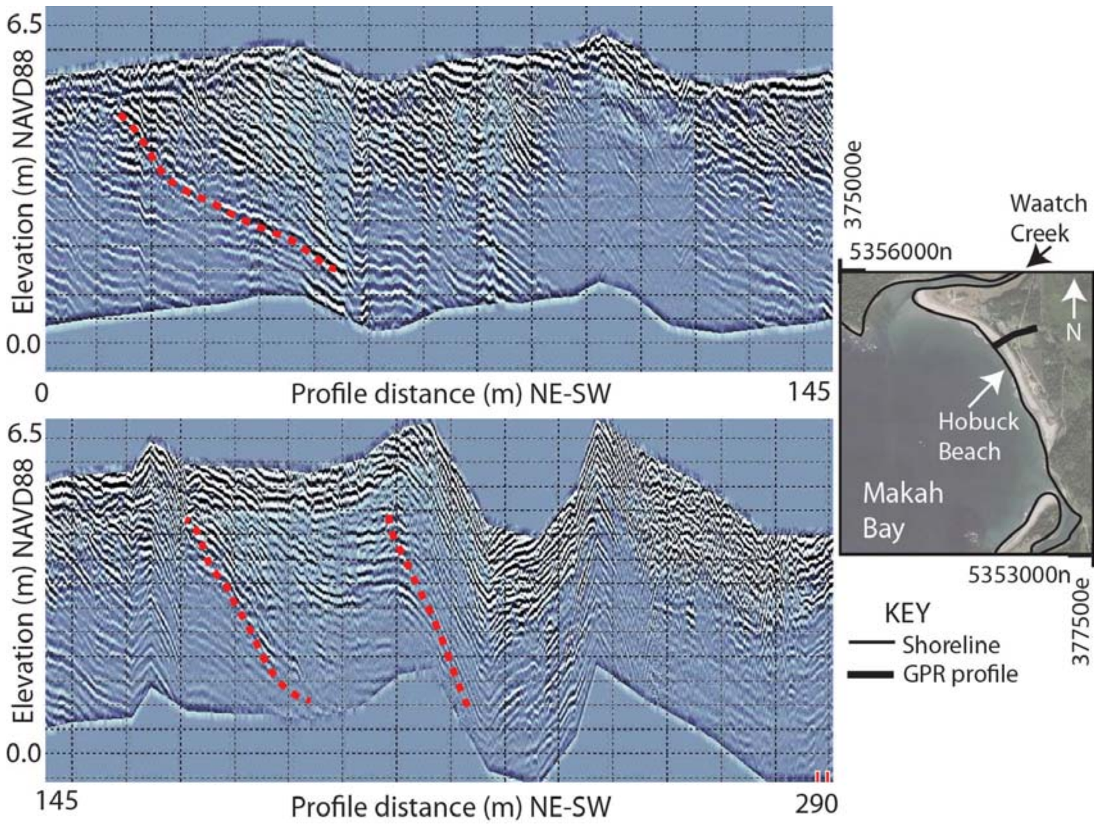

Figure 5. Across-shore (northeast to southwest) GPR profile (250 MHz) taken at Hobuck Beach, Washington (SW endpoint UTM 0376622e, 5355274n). The cross-section shows progradation of an intact beach plain east to west (two parts: upper part 0–145 m distance and lower part 145–290 m distance) with seaward dipping beach face reflections, to 6 m depth. Figure inset shows approximate profile orientation across the beach plain. Prograded beach deposits reach ~5.5–6.0 m elevation (NAVD88) as surveyed into NOAA GPS benchmark E4-GPS-BBCJ13 (Peterson et al., 2013). Three very-weak retreat scarps (dashed lines) are traced into the shallow subsurface at 30, 170 and 210 m profile distances. Their origins are unknown and no radiocarbon or OSL dates are currently available for the Hobuck Beach plain. The single GPR profile is from Peterson and Butler, unpublished data (2011).

3 and 4) are interpreted to have originated from sustained catastrophic marine surge(s), as produced by Cascadia nearfield paleotsunamis (Clague and Brobowsky, 1994; Clague et al., 2000; Peterson et al., 2013). The dune ridge is isolated from outwash deposits in the late Pleistocene terraces and/or any other landward sources of gravel. The fine gravel deposits (5–15 cm thickness), including pebbles 1–2 cm in diameter (Table 2), were apparently deposited by paleotsunami flows (> 0.5 m depth) that exceeded 9.0 m elevation at site SP-8. Shallow soil pits in landward terrace sites, SP9 and SP10, also contained minor abundances of well-rounded pebbles that were hosted in bioturbated loess at 9–10 m elevation. Underlying sources of terrace outwash gravels cannot be ruled out for the pebble origins in SP9 and SP10. However, the lack of any pebbles in loess deposits from higher elevation sites, SP11 and SP12, respectively, at 11 and 12 m elevation, does place constraints on the possible maximum runup of gravel-bearing tsunami surges. Such high-velocity surges that did leave gravel at 9.0 m elevation in SP8 did not reach 11 m elevation in SP11 in the most proximal terrace flats in North Sand Point.

The age of the dune ridge in the prograded beach plain, between ~1.5 ka and ~0.6 ka, restricts the paleotsunami runup event to one of the last 3–4 paleotsunamis in the region (Clague and Brobowsky, 1994; Peterson et al. 2013). The event at ~1.3 ka has, by far, the greatest recorded inundation in the Waatch Creek wetlands (Figure 1). We attribute the paleotsunami deposit that overtopped the high dune ridge crest (SP8) to the Cascadia paleotsunami at ~1.3 ka (Figure 3). No soil A-horizon interbeds or paleosols occurred in the stratified gravel at SP8 (Figure 4). The age of the stone net weight (Figure 6) in the paleotsunami layer at SP3/4 must predate the age of the ~1.3 ka tsunami that remobilized the stone artifact and the hosting pebbly fine sand. The net weight artifact at ~20 cm size is out of hydrodynamic equivalence with the 1–2 cm diameter pebbles that surrounded it. Therefore, we do not believe that the artifact was transported landward over the dune ridge crest with the pebbles, but rather that it was eroded from the nearby terrace midden area 45-CA-201 and rolled down the terrace riser, possibly by paleotsunami backwash. The paleotsunami post-dates the onset of beach plain progradation and so therefore it also post-dates the midden occupation (~2.3–1.6 ka) (Tables 1 and 3). The stone net weight was reburied on site, but off to the side of the published cross-section, by the supervising archaeologists during fieldwork.

At least two other anomalous gravel layers were found at depths of 1.5 m and 0.8 m, respectively in SP5 and SP1/2, located seaward of the abandoned foredune ridge. It is not known whether the two anomalous gravel layers are correlated or whether they reflect two different marine-surge events. The gravel layer in SP1/2 post-dates the minimum OSL age of 0.6 ka (Table 3). We suspect that these anomalous gravel layers in SP1/2 and SP5 might represent paleotsunami deposits that derived from younger and smaller paleotsunami runups associated with Cascadia ruptures at ~1.1 and 0.3 ka, after the larger paleotsunami at ~1.3 ka (Peterson et al., 2013). Additional work is required to confirm the possible paleotsunami origins of the anomalous gravel layers in SP1/2 and SP5 at the west end of the North Sand Point cross-section.

Dynamic Conditions of Beach Sand Recycling and Potential Future Erosion

The accumulations of sand in the prograded beach plains located on both sides of Sand Point (Figure 2) confirm longshore trapping of net northward littoral drift in the southwest facing pocket beaches of the Olympic Peninsula (Swartz et al., 1985). The restricted ages of the North Sand Point beach plain deposits (~1.5–0.6 ka) both 1) confirm ongoing net-northward littoral drift during latest Holocene time and 2) imply episodic or non-continuous conditions of beach sand accumulation in the small pocket beach. The multiple ages of grain bleaching from OSL samples UW2470 and UW2469 (Table 2) reinforce the appearance of long-term beach instability in the study area. Minor components of sand grain ages range from 11.1 ± 8.3 ka to 4.7 ± ka. The minor components substantially pre-date the central ages of the useable grain populations (2.68 ± 0.29–1.19 ± 0.12 ka) and the minimum ages of the youngest grains (1.32 ± 0.19 and 0.64 ± 0.09 ka) in the North Sand Point cross-section.

A complex history of beach sand burial, erosion, and remobilization(s) with or without partial bleaching(s) is required to account for the spread of grain OSL ages in the beach plain deposits in North Sand Point. The apparent episodic conditions of sand supply and remobilization are not unexpected in the high wave energy environments of the Pacific Ocean coastline. The sand grain remobilization(s) demonstrate episodic erosion throughout late-Holocene time (5–0 ka). Furthermore, the lack of net accumulation after 0.6 ka in the North Sand Point beach plain implies near-term vulnerability of the small pocket beach and the associated backshore cultural sites, such as the one adjacent to SP1/2 (Figure 3), to potential future beach erosion. The threat of episodic beach erosion and associated loss of some archaeological materials in the Olympic National Park coastline (Wessen, 2003) will increase with time, particularly in the face of predicted future global sea level rise (Peterson, 2012) and/or changes in regional wave climate (Ruggiero et al., 2010b) in the Pacific Northwest region.

Summary and Future Work

The very small pocket beach in North Sand Point is well situated to address several important geomorphic questions about beach sand supply, neotectonics, backshore archaeological sites,

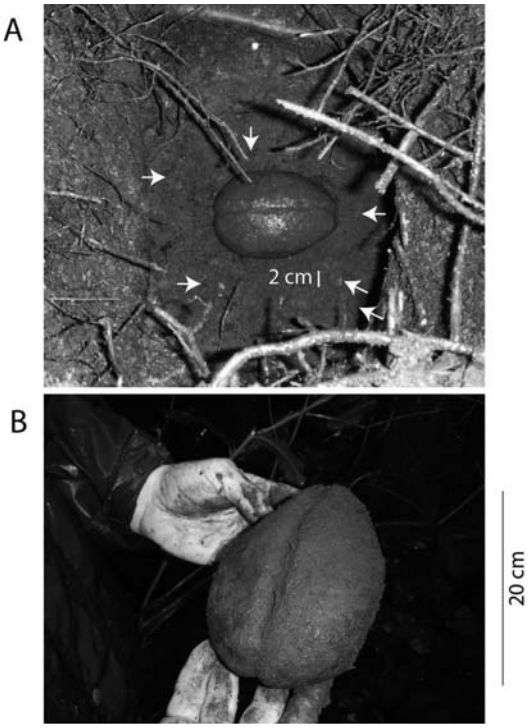

Figure 6. Part A: Stone net weight in a tsunami pebble layer, as revealed below the soil litter layer in a shallow soil pit adjacent to SP3/4. Paleotsunami pebbles (white arrows) reach 2 cm diameter, as exposed in fine dune sand that hosts the paleotsunami layer and the net weight. Part B: Released stone net weight (20 cm maximum dimension) shows hand-pecked groove (longitudinal).

There is no evidence of local faults uplifting the narrow beach plain (~120 km width) in the North Sand Point pocket beach. The maximum elevations of coarse beach-sand deposits (~5–6 m elevation) are traced from the foot of the abandoned terrace sea cliff to the modern beach backshore. The anomalously high sand ridge at 9 m elevation is not due to tectonic uplift but rather to eolian dune deposition above the beach sand facies. The initiation of beach plain progradation at ~1.5 ka does not directly coincide with known Cascadia megathrust ruptures, but it could be coeval with a broad period of interseismic uplift between regional ruptures at ~1.7 and ~1.3 ka. Additional work is needed to establish whether records of coseismic beach retreat and interseismic beach recovery are recorded in the Sand Point locality.

Anomalous gravel deposits that locally drape the top of the abandoned foredune ridge (9.0 m elevation) are interpreted to represent catastrophic marine surge deposition from the Cascadia paleotsunami at ~1.3 ka. Tsunami pebble transport is not apparent above 11.0 m elevation in the landward terrace flats, thereby restricting the maximum-recorded runup of gravel-bearing flows to 10 ± 0.5 m elevation. The paleotsunami surge(s) at ~1.3 ka would have post-dated the occupation of the 45-CA-201 midden site, which was abandoned by ~1.6 ka. It is not known if subsequent paleotsunamis inundated cultural sites on the prograded beach plain, such as the one adjacent to SP1/2, during later occupations (Figure 3).

Apparent episodic erosion and reworking of littoral sediments in the high-wave energy conditions of the Sand Point locality are indicated by 1) the brief period of recorded beach plain progradation, 2) the termination of net progradation at 0.6 ka, and 3) a variety of beach grain bleaching ages in North Sand Point OSL samples. The bleaching ages of major and minor components, ranging from 11.1 ka to 2.3 ka, predate the onset of beach plain progradation at ~1.5 ka. Those components represent sand grains that were bleached under previous conditions of subaerial exposure, presumably from reworked beach deposits. The short-term instabilities of the small pocket beaches in Olympic National Park heighten concerns and potential future erosion in the Pacific Ocean coastline of the Olympic Peninsula. A brief period of net beach plain progradatation (~1.5–0.6 ka) in the pocket beach, located on the south side of Point Alava (Figure 1) confirms net northward littoral drift in the region during latest-Holocene time. The nearest large coastal river, the Quillayute River, is located > 25 km south of the study area. The intervening narrow beaches, rocky shorelines, and multiple headlands, imply that northward sand transport extends to the inner-shelf but it is supply limited. Beach sand tracer studies, utilizing heavy minerals or sand source signatures, might help to reveal the source(s) of sand, such as local rivers, eroded terrace deposits, and/or the Columbia River, moving northward along the rugged coastline of the Olympic Peninsula.

about the potential loss of archaeological sites and materials to future beach erosion following predicted global sea level rise and/or changes in regional wave climate. Given these concerns, an inventory of the most vulnerable sites in prograded pocket-beach plains could be initiated in the west coast of the Olympic Peninsula.

Acknowledgements

Gary Wessen, Wessen Associates Inc., supervised auger core site selection and hand test-pit sampling. Dave Conca and Li Clinton, Olympic National Park, assisted with permitting, logistical support, and field communications. Mary Robins and Dan Anderson assisted with paleotsunami gravel sampling. Tracy Handrich performed the beach, dune, and paleotsunami deposit mechanical sieving. J. Tait Elder, Dianna Woolsey, Katie Mohlenhoff, Shoshana Rosenberg, Joshua Dinwiddie, Tammy Yasrobi, Anthony Hofkamp, Leslie Crippen and Andy Huff, among others of the Portland State University Geoarchaeology course (2011) assisted with auger core logging and data compilation. Sehar Sheikh assisted with OSL dating. The office of Research and Strategic Partnerships at Portland State University provided support for the OSL dating that was performed for this investigation.

Literature Cited

Atwater, B. F., M. P. Tuttle, E.S. Schweig, C. M. Rubin, D. K. Yamaguchi, and E. Hemphill-Haley. 2004. Earthquake recurrence, inferred from paleoseismology. *In* Gillespie A. R., S. C. Porter, and B. F. Atwater (editors), The Quaternary Period in the United States, Elsevier, Amsterdam. Pp. 331-350.

Bird, E., and M. Swartz. 2000. Shore platforms at Cape Flattery, Washington. Washington Geology 28:10-15.

Clague, J. J., and P. T. Bobrowsky. 1994. Tsunami deposits beneath tidal marshes on Vancouver Island, British Columbia. Geological Society of America Bulletin 106:1293-1303.

Clague, J. J., P. T. Bobrowsky, and I. Hutchinson. 2000. A review of geological records of large tsunamis at Vancouver Island, British Columbia, and implications for hazard. Quaternary Science Reviews 19:849-863.

Feathers, J., and S. Sheikh. 2012. Luminescence dating of sediments from Sand Point on the Olympic Peninsula, Washington. Report to the Olympic National Park, United States National Park Service. University of Washington Luminescence Dating Laboratory, Seattle, WA.

Galbraith, R. F, and R. G. Roberts. 2012. Statistical aspects of equivalent dose and error calculation and display in OSL dating: an overview and some recommendations. Quaternary Geochronology 11:1-27.

Meyers, R. A., D. G. Smith, H. M. Jol, and C. D. Peterson. 1996. Evidence for eight great earthquake-subsidence events detected with ground-penetrating radar, Willapa barrier, Washington. Geology 24:99-102.

Mosher, D. C., and A. T. Hewitt. 2004. Late Quaternary deglaciation and sea-level history of eastern Juan de Fuca Strait, Cascadia. Quaternary International 121:23-39.

Pazzaglia, F. J., and M. T. Brandon. 2001. A fluvial record of long-term steady state uplift and erosion across the Cascadia forearc high, western Washington State. American Journal of Science 301:385-431.

Peterson C. D, K. M. Cruikshank, M. E. Darienzo, G. Wessen, V. Butler, and S. Sterling. 2013. Coseismic subsidence and paleotsunami runup records from latest Holocene deposits in the Waatch Valley, Neah Bay, northwest Washington, USA: Links to great earthquakes in the northern Cascadia margin. Journal of Coast Research 29:157-172.

Peterson, C. D. 2012. Impacts of predicted global sea level rise on Oregon beaches and tidelands: Planning for global sea level rise in Oregon, USA. Just Cerfing, Coastal Education and Research Foundation, 3:1-17. Available online at http://cerf-jcr.com/Just-Cerfing-June-2012.pdf (accessed 11 May 2014).

Peterson, C. D., G. H. Grathoff, F. Reckendorf, D. Percy, and D. M. Price. 2014. Late Pleistocene coastal loess deposits of the central west coast of North America: Terrestrial facies indicators for marine low-stand intervals. Aeolian Research 12C:47-64.

Peterson, C. D., P. L. Jackson, D. J. ONeil, C. L. Rosenfeld, and A. J. Kimerling. 1990. Littoral cell response to interannual climatic forcing 1983-1987 on the central Oregon coast, USA. Journal of Coastal Research 6:87-110.

Peterson, C. D., P. D. Komar, and K. F. Scheidegger. 1985. Distribution, geometry and origin of heavy mineral placer deposits on Oregon beaches. Journal of Sedimentary Petrology 56:67-77.

Peterson, C. D., E. Stock, R. Hart, D. Percy, S. W. Hostetler, and J. R. Knott. 2009. Holocene coastal dune fields used as indicators of net littoral transport: West Coast, USA. Geomorphology 116:115-134.

Peterson, C. D., S. Vanderburgh, M. C. Roberts, H. M. Jol, J. P. Phipps, and D. C. Twichell. 2010. Composition, age, and depositional rates of Holocene shoreface deposits under barriers and beach plains of the Columbia River littoral cell, USA. Marine Geology 273:62-82.

Ruggiero, P. M. Buijsman, G. M. Kaminsky, and G. Gelbenbaum. 2010a. Modeling the effects of wave climate and sediment supply variability on large-scale shoreline change. Marine Geology 273:127-140.
Ruggiero, P., P. D. Komar, and J. C. Allan. 2010b. Increasing wave heights and extreme value projections: The wave climate of U.S. Pacific Northwest. Coastal Engineering 57: 539-552.
Snavely, P. D., Jr., Raw, W. W., Pearl, J. E., Niem, A. R., MacLeod, N. S., Minasian, D. L., 1993. Geologic Map of the Cape Flattery, Clallam Bay, Ozette Lake, and Lake Pleasant quadrangles, northwestern Olympic Peninsula. U.S. Geological Survey Miscellaneous Investigations Series Map I-1946, Map. Scale 1:48:000. Available online at http://ngmdb.usgs.gov/Prodesc/proddesc_10020.htm (accessed 14 December 2014).
Swartz, M. L., M. James, and H. S. Bronson. 1985. Net shore-drift along the Pacific Coast of Washington State. Shore and Beach 53: 21-33.
Thackray, G. D. 1998. Convergent-margin deformation of Pleistocene strata on the Olympic coast of Washington, USA. *In* I. S. Stewart and Vita-Finzi (editors), Coastal Tectonics. Geological Society, London, Special Publications 146:199-211.
Wessen, G. 1984. A Preliminary Report of Archaeological Investigations at 45CA201, a "Second Terrace" Shell Midden near Sand Point, Olympic National Park, Washington. A report prepared for the National Park Service Pacific Northwest Regional Office by Wessen & Associates. Burien, WA.
______. 1993. Archaeological Activities at and near Sand Point (45CA201), Olympic National Park, Washington. A report prepared for the National Park Service Pacific Northwest Regional Office by Wessen & Associates, Burien, WA.
______. 2003. An assessment and plan for a program of studies addressing prehistoric archaeological sites associated with paleoshorelines on the Olympic Coast of Washington. Prepared for the Olympic Coast National Marine Sanctuary, Port Angeles Washington, and the Makah Cultural Research Center, Neah Bay, WA.
West, D. O. and D. R. McCrumb. 1988. Coastline uplift in Oregon and Washington and the nature of Casadia subduction zone tectonics. Geology 16:169-172.

Received 31 January 2014
Accepted for publication 09 September 2014